Radiation Pattern Synthesis from Various Shaped Reflectors Base on PO and PTD Methods for Point-to-Multipoint Applications

VANVISA THAIVIROT, PIYAPORN KRACHODNOK, AND RANGSAN WONGSAN
School of Telecommunication Engineering, Institute of Engineering
Suranaree University of Technology
111 University Avenue, Muang District, Nakhon Ratchasima, 30000
THAILAND
Email : priam@sut.ac.th, rangsan@sut.ac.th

Abstract: - This paper presents the shaped reflector antenna by using backscattering technique to achieve the completely broad-beam radiation pattern. The radiation synthesis method for shaped reflector that has to illuminate a predefined circular area are presented by using a variety of discretization of elementary geometrical functions such as, triangular, quadratic, circular, guassian, cosine, squared cosine, parabolic and hyperbolic distributions. The antenna characteristics i.e., maximum ripple level, maximum gain, and half-power beamwidth (HPBW) of the variety of shaped reflectors are analytically determined by using physical optics (PO). These shapes reflector will be discussed on merit and demerit to choose for utilization in wireless local area network (wireless LAN). The reflector which has appropriate characteristics for indoor wireless LAN in very large room will be analyzed detail by introducing the fringe wave (FW) in physical theory of diffraction (PTD). Having confirmed the validity of this approach, the X-band antenna prototype is designed and developed. The proposed antenna is tested experimentally and shows good performance.

Key-Words: - PO, PTD, shaped reflector, radiation pattern synthesis, broad-beam antenna, wireless LAN

1 Introduction

In recent years, wireless communications systems such as wireless local area network (wireless LAN) and Bluetooth are being rapidly adopted. Therefore, specific antenna system was researched and developed to comply with requirements dictated by such applications. At present, the popular antennas for indoor wireless LAN access points are linear dipole, slot array, and microstrip antenna [1]-[4]. These antennas will be usually placed at the wall of rooms or buildings. However, most kinds of these antennas have omnidirectional pattern, therefore, they are not suitable for field radiating in the large room because of power loss in unnecessary directions such as outside of room. This argues, if we can design an antenna to illuminate a predefined circular area without substantial spatial variation, it will have more efficient for field radiating. The proposed antenna will be installed on the center point of ceiling in very large room. Consequently, the all client computers, which are in this room, will be connected to the access point of wireless LAN through the only one antenna, as shown in Fig.1. Moreover, interesting characteristics of the proposed antenna can also be utilized for the low-earth orbit (LEO) satellite in space communication.
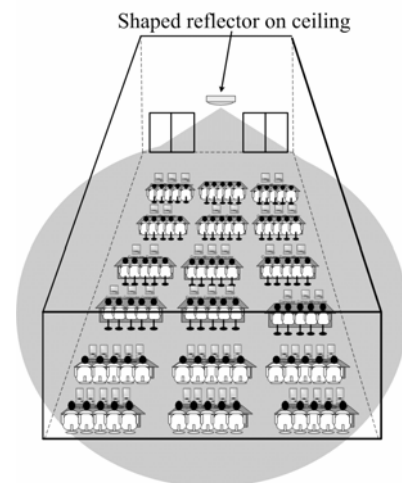

Fig. 1 Shaped reflector for wireless LAN large-scale indoor base station.

To meet this requirement, we focused our attention on shaped reflector antenna. In following, we review the categories of shaped reflector antennas. The highly shaped-beam antenna was first developed to give approximately uniform coverage of the earth from satellite antenna [5]. Recently, the similar requirement but different application that is, the indoor high speed data transmission: wireless LAN operating in the millimeter wave, again

attracts considerable attentions [6]-[9]. Due to the critical specification in link budget, the transmitted power has to be efficiently distributed over the coverage; the spatial fluctuation of the field strength has to be as small as possible (within 6 dB) within the defined coverage area, whereas outside the coverage the field strength has to fall off rapidly. A shaped reflector antenna for 60-GHz indoor wireless LAN access point was developed [7]-[8]. A circular footprint having the deviation from the average field strength less than 2.5 dB in the far field was reported [8]. However, shaped reflector antenna have to design a new shaped reflector always in order to generate the new shaped beam for different coverage specifications. Therefore, if we can synthesize variety of shaped reflector for wide variety of different coverage area, it will be easy to design shaped reflector for use in wireless LAN, LEO satellite or other applications.

In this research, the antenna under consideration is shaped reflector by using backscattering technique to achieve the completely broad-beam radiation pattern. The present reflectors are defined surfaces by using the various functions of elementary geometries i.e., triangular, quadratic, circular, guassian, cosine, squared cosine, parabolic and hyperbolic surface shapes. The antenna characteristics i.e., maximum ripple level, maximum gain, and half-power beamwidth (HPBW) of the variety of shaped reflectors are analytically determined by using physical optics (PO). Surprisingly, there is no research for applying PO method to analyze radiation pattern of reflector by using the elementary geometrical functions. In addition, each shapes of reflector will be discussed on merit and demerit to choose for utilization in wireless communication. Moreover, the reflector which has appropriate characteristics for indoor wireless LAN in very large room will be analyzed detail by introducing the fringe wave (FW) in physical theory of diffraction (PTD), the hybrid method gives fields which are numerical analysis to exact one for practical problems. Finally, the fabrication and measurement of the proposed reflector antenna are investigated its radiation characteristics.
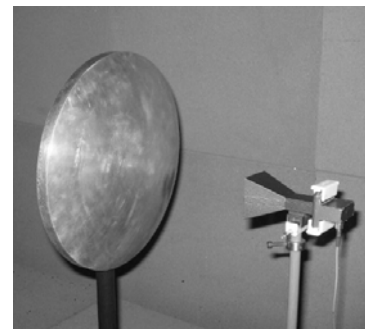
2 Antenna Configuration

As shown in Fig.2, the antenna under consideration contains reflector with diameter denoted as D, which are determined surfaces by using functions of elementary geometries from Table 1 and distribution of the function as illustrated in Fig.4. A standard X-band horn feed is placed at a position that estimates illumination the reflector edge with -10 dB when

compared with the illumination at the center of the reflector. The figure of -10 dB edge illumination may be considered as a compromise between the amount of spillover, on the one hand, and efficient illumination of the reflector surface on the other.
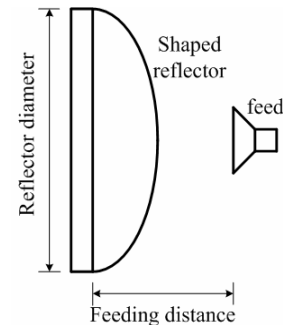
(a)

(b)

Fig. 2 Antenna configuration with shaped reflector.

The radiation pattern of standard X-band horn as shown in Fig.3 which relative power at the angle ±28° in E-plane and the angle ±41° in H-plane provide -10 dB edge illumination on reflector with diameter $D = 10\lambda$ and provides feeding length about 28 cm in E-plane and 17 cm in H-plane.
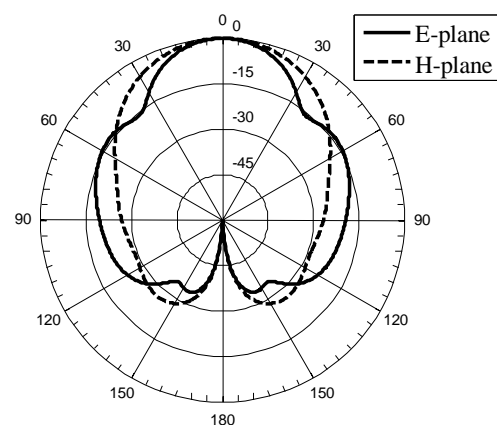

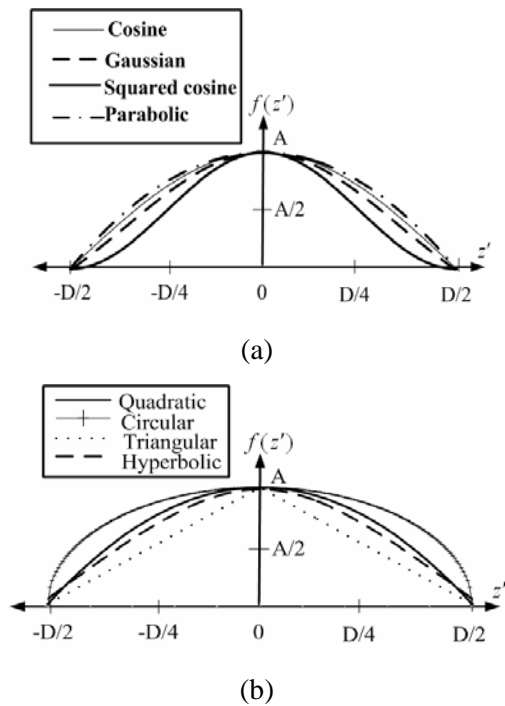Fig. 3 Radiation pattern of standard X-band horn.

(a)

(b)

Fig. 4 Various elementary geometrical functions.

Table 1
Formulations of elementary geometrical function.

Distributed functions	Formulations	Shapes of reflector
Triangular	$f(x,y) = A\left(1 - \dfrac{2}{D}\sqrt{x^2+y^2}\right)$	
Quadratic	$f(x,y) = A\left[1 - \left(\dfrac{2}{D}\sqrt{x^2+y^2}\right)^2\right]$	
Circular	$f(x,y) = A\sqrt{1 - \left(\dfrac{2}{D}\sqrt{x^2+y^2}\right)^2}$	
Gaussian	$f(x,y) = Ae^{-\left(\frac{2}{D}\sqrt{x^2+y^2}\right)^2}$	
Cosine	$f(x,y) = A\cos\left(\dfrac{\pi}{D}\sqrt{x^2+y^2}\right)$	
Squared cosine	$f(x,y) = A\cos^2\left(\dfrac{\pi}{D}\sqrt{x^2+y^2}\right)$	
Parabolic	$f(x,y) = \left(\sqrt{x^2+y^2}\right)^2 / 4f$	
Hyperbolic	$f(x,y) = a\sqrt{1 + \dfrac{\sqrt{x^2+y^2}}{b}}$	

The different elementary geometrical functions as shown in Fig.4, z' is function of variable x and y where $-D/2 \le z' \le D/2$ and $z' = \sqrt{x^2+y^2}$. A is the depth of the reflectors.

3 Theory

Radiation pattern analysis is a key technology in antenna design. One of technique that has been widely used in the analytical determination of the radiation patterns of reflector antennas is physical optics (PO). It has the popularity due to its simplicity in the algorithm and regularity of predicted fields. PO, which is characterized by the surface radiation integrals of approximate secondary induced currents, neglect the diffraction effects from truncating edges as well as the curvature of the surface in defining the currents. High frequency (HF) diffraction is known as local phenomena, and only part of the scatter contributes to the field such as the edge, corner and specular reflection point etc. Geometrical Theory of Diffraction (GTD), Uniform Theory of Diffraction (UTD) and Physical Theory of Diffraction (PTD) are methods relying upon the local properties of high frequency diffraction. GTD became an even more effective tool because of its accuracy and simplicity. However, the singularities of GTD at caustics still exist in the uniform versions [10]. While other technique developed at the same time as GTD is PTD pioneered by Ufimtsev [11]. Two important modifications to the original PTD have been achieved. The first one is the application of the concept of equivalent edge current (EEC) which eliminates the caustic singularities in the original ray tracing PTD. The second one is an extension for observation angles, which are not on the positions of angle of Keller's cone. Ando's modified PTD is one modification that uses the concept of EEC [12]. Mitzner, on the other hand, did not use EEC explicitly but rather expressed the PTD correction fields in terms of incremental length diffraction coefficients (ILDC) [13]. Michaeli's work is the third modified PTD and will be utilized to evaluate the radiation pattern of backscattering reflector in this paper. He derived the GTD quivalent edge currents by asymptotically reducing the surface to edge integral [14]. Later, Michaeli evaluated the fringe current radiation integral over the "ray coordinate" instead of over the "normal coordinate". This improvement using such techniques corrected many of the singularities in Mitzner's ILDC [15].

The PTD is an integrative technique in which the PO current on a discontinuous perfect conductor surface is refined by the addition of a so-called "nonuniform" component due to the presence of the (edge) discontinuity. The analytical procedure is shown in Fig.5.
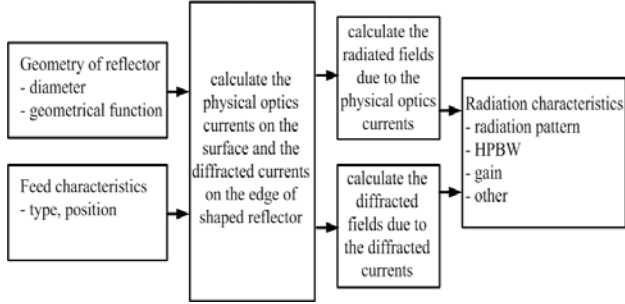

Fig. 5 Analytical procedure.

The PO expression for the electric fields radiated from the reflector surface is given by

$$\bar{E}^{PO}(\theta,\phi) = -j\omega\mu \frac{e^{-jkr}}{4\pi r}\left(\hat{1}-\hat{r}\hat{r}\right)\cdot\iint_{\Sigma'}(2\hat{n}\times\bar{H}^{i})e^{jk\hat{r}\cdot\bar{r}_{\sigma'}}\,d\sigma', \quad (1)$$

where Σ' is a reflector surface, $2\hat{n}\times H^{i}$ is the PO current, and $\hat{n}$ is a unit normal to the surface as shown in Fig.6. The dyad $(\hat{1}-\hat{r}\hat{r})$ serves to extract the transverse (to $\hat{r}$) component of the surface integral.
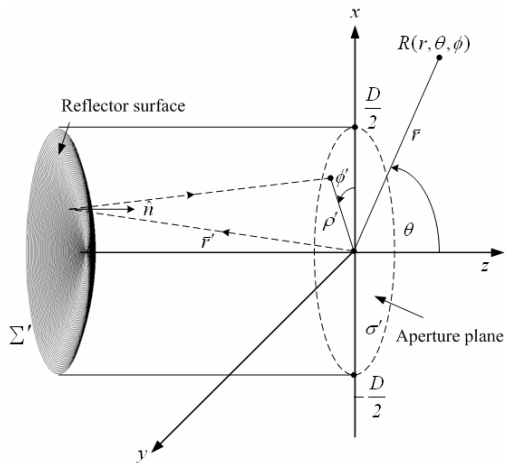

Fig. 6 Three-dimensional geometry of a reflector.

In Mitzner's, Michaeli's and Ando's methods, the total scattered field $\bar{E}^{PTD}$ is constructed by adding a diffracted field $\bar{E}^{d}$ to the physical optics field $\bar{E}^{PO}$ in (1) [16] as

$$\bar{E}^{PTD} = \bar{E}^{PO} + \bar{E}^{d}. \quad (2)$$

The diffracted field due to an edge discontinuity C is given for the observation point by the radiation integral

$$\bar{E}^{d} \cong jk\int_{C}\left[ZI^{f}(\bar{r}')\hat{s}\times(\hat{s}\times\hat{e}) + M^{f}(\bar{r}')\hat{s}\times\hat{e}\right]G(\bar{r}',\bar{r})dl \quad (3)$$

In Michaeli's equivalent edge currents, the final expressions for I^{f} and M^{f} [17] as

$$I^{f} = \left(E_{o}^{i}\cdot\hat{e}\right)\frac{2j}{Zk\sin^{2}\beta'}\frac{\sqrt{2}\sin\left(\frac{\phi'}{2}\right)}{\cos\phi'+\mu}\left[\sqrt{1-\mu}-\sqrt{2}\cos\left(\frac{\phi'}{2}\right)\right]$$
$$+\left(H_{o}^{i}\cdot\hat{e}\right)\frac{2j}{k\sin\beta'}\frac{1}{\cos\phi'+\mu}\cdot[\cot\beta'\cos\phi'+\cot\beta\cos\phi \quad (4)$$
$$+\sqrt{2}\cos\left(\frac{\phi'}{2}\right)\left(\mu\cot\beta'-\cot\beta\cos\phi\right)\left(1-\mu\right)^{-\frac{1}{2}}],$$

$$M^{f} = \left(H_{o}^{i}\cdot\hat{e}\right)\frac{2jZ\sin\phi}{k\sin\beta\sin\beta'}\frac{1}{\cos\phi'+\mu}$$
$$\times\left[1-\sqrt{2}\cos\left(\frac{\phi'}{2}\right)\left(1-\mu\right)^{-\frac{1}{2}}\right], \quad (5)$$

where

$$\mu = \frac{\cos\gamma-\cos^{2}\beta'}{\sin^{2}\beta'}, \; G(\bar{r}',\bar{r}) = \frac{e-jks}{4\pi s},$$

$$\cos\gamma = \sin\beta'\sin\beta\cos\phi+\cos\beta'\cos\beta,$$

$$\beta = \pi-\cos^{-1}(\hat{s}\cdot\hat{e}), \; \beta' = \pi-\cos^{-1}(\hat{s}'\cdot\hat{e}),$$

$$\hat{\phi} = \frac{\hat{s}\times\hat{e}}{\|\hat{s}\times\hat{e}\|}, \; \hat{\phi}' = \frac{\hat{e}\times\hat{s}'}{\|\hat{e}\times\hat{s}'\|}, \; \hat{\beta} = \hat{s}\times\hat{\phi}, \; \hat{\beta}' = \hat{s}'\times\hat{\phi}',$$

$$\phi = \begin{cases} \cos^{-1}(\hat{n}\cdot\hat{\phi}) & \hat{t}\cdot\hat{\phi}\leq 0 \\ 2\pi-\cos^{-1}(\hat{n}\cdot\hat{\phi}) & \hat{t}\cdot\hat{\phi}>0 \end{cases},$$

$$\phi' = \begin{cases} \cos^{-1}(\hat{n}\cdot\hat{\phi}') & \hat{t}\cdot\hat{\phi}'\leq 0 \\ 2\pi-\cos^{-1}(\hat{n}\cdot\hat{\phi}') & \hat{t}\cdot\hat{\phi}'>0 \end{cases}.$$

$\hat{s}'$ is the unit vector from the feed to the edge, $\hat{s}$ is the unit vector from the edge to the observer, k is the wavenumber of the incident wave, Z is the intrinsic impedance of the medium, $\bar{r}$ and $\bar{r}'$ are the position vectors of the observation point and a point on edge C, respectively. Where dl is the increment of arc length l along edge of reflector C, $\hat{e} = -\bar{r}'/\|\bar{r}'\|$ is the unit vector tangent to the edge, $\hat{n}$ is the unit normal vector to the edge, $\hat{t} = \hat{e}\times\hat{n}$ is the unit tangent vector outward from the edge to surface, $\bar{E}_{o}^{i}$ and $\bar{H}_{o}^{i}$ denote the incident electric and

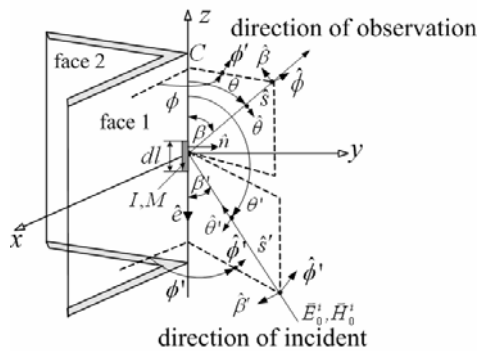magnetic field vector, respectively, as shown in Fig.7.



Fig. 7 Wedge scattering geometry.

4 Numerical Results

4.1 Radiation pattern synthesis

In practice, it is often necessary to design an antenna system that yields desired radiation characteristics. For example, a very requirement for indoor wireless LAN application are the pattern to exhibit a desired distribution, wide beamwidth, high gain, low ripple level and so forth. Therefore, radiation pattern synthesis will be utilized to help choosing the appropriate reflector shape for indoor wireless LAN application or the LEO satellite in space communication.

In this paper, we synthesize the radiation pattern from the various shapes of reflector with diameter $D = 30$ cm and a standard X-band horn feed for frequency 10 GHz, which is placed at a position that estimates illumination the reflector edge with -10 dB when compared with the illumination at the center of the reflector. This frequency is chosen because our experimental equipment can be use. The configurations of variation reflectors are given by using functions of elementary geometries from Table 1. The radiation pattern for each reflector shape is calculated by using PO as expressed in (1) and their simulated results are shown together in Fig.8.

Radiation pattern as shown in Fig.8 are different due to curve of each reflector which provides different characteristics such as ripple level, HPBW, and maximum gain. From the characteristics of various reflector shapes in Table 2, it is obvious to see that the ripple level of the squared cosine shaped reflector has the maximum ripple and followed, in order, by hyperbolic, gaussian, parabolic, quadratic, cosine and circular shapes, at 2.66 dB, 1.24 dB, 1.06 dB, 0.85 dB, 0.83 dB, 0.79 dB, 0 dB respectively. However, ripple on the pattern of triangular shape has appeared between two main

beams whereas on the top of the main beams are 0.77 dB. The HPBW of eight shaped reflectors in the second column of Table 2, for average consideration, it is apparent that the gaussian shaped reflector has the widest beamwidth and followed, in order, by hyperbolic, squared cosine, cosine, quadratic, parabolic and circular shapes, which are $132°$, $120°$, $118°$, $99°$, $98°$, $96°$ and $58°$, respectively, while HPBW of triangular shape is about $18°$ on each beam. Finally, the maximum gain of eight shaped reflectors are compared and shown in the last column of Table 2. It is found that the circularly shaped reflector has the maximum gain and followed, in order, by quadratic, parabolic, cosine, hyperbolic, gaussian and squared cosine shapes, which are 10.28 dB, 7.76 dB, 7.25 dB, 6.95 dB, 6.12 dB, 6.02 dB and 4.53 dB, respectively, while the maximum gain of triangular shape is 8.71 dB (see at each top of beam). From the simulated data in Table 2, it is noted that, both HPBW and the maximum gain depend on ripple level and gain of each reflector shape is not coincided with the HPBW.
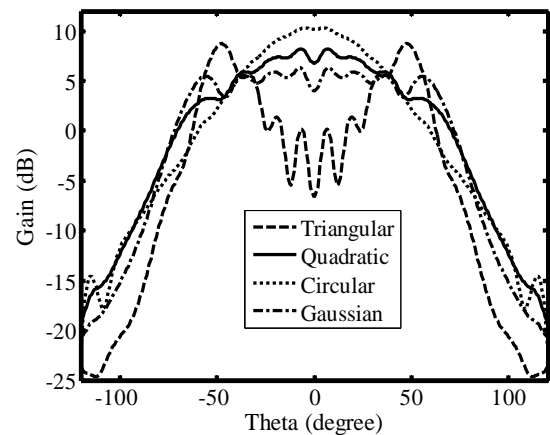
(a)
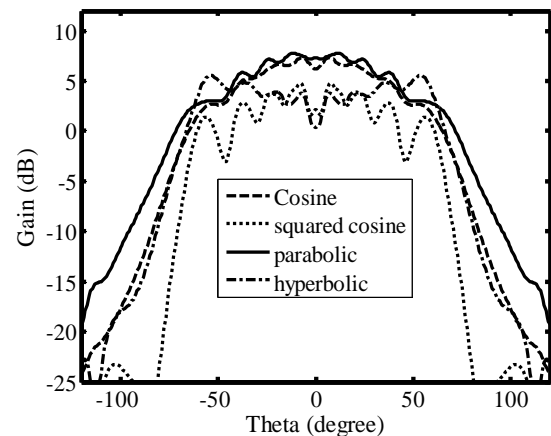
(b)

Fig. 8 Radiation patterns in H-plane.

Table 2
Radiation characteristics for various shaped reflectors.

Reflectors shapes	Ripple level (dB)	HPBW (degree)	Maximum gain (dBi)
Triangular	0.77	18	8.71
Quadratic	0.83	98	7.76
Circular	0.00	58	10.28
Gaussian	1.06	132	6.02
Cosine	0.79	99	6.95
Squared cosine	2.66	118	4.53
Parabolic	0.85	96	7.25
Hyperbolic	1.24	120	6.12

From all the aforementioned of radiation characteristics, it can be summarized that these reflector shapes can be chosen according to the characteristic requirements in practical applications. For example, if the widest HPBW is required for radiating in indoor large-scale wireless LAN application, the gaussian shape of reflector is the most appropriate. Whereas we need the reflector, which yields very high gain for the center of large room, the circularly shaped reflector should be utilized. However, the remaining shapes have intermediate characteristics between gaussian and circular shapes, while some surface shapes yield the high ripple level. From view graphs of radiation patterns in Fig.8, it is easy to find the proper reflector at which meet the requirement of the characteristic specifications. To get more advantages in one characteristic while sacrificing the merit of another characteristic in the same surface shape is difficult to avoid. The designer must compromise among the entire characteristics of reflector are an alternative way to keep all acceptable properties in one reflector. In this paper, authors decide to choose quadratic reflector to construct antenna model at 10 GHz for indoor wireless LAN application because it has appropriate characteristics i.e., low ripple level (smooth power level) and wide HPBW (wide coverage area). Moreover, it yields rather high gain than the common antennas, which are nowadays used for indoor wireless LAN access point. However, the decision of reflector shapes selection depend desired radiation characteristics to utilize for each application.

4.2 Diffraction Analysis by Using PTD

The synthesis radiation pattern by using PO described in the previous section will be analyzed detail by introducing the fringe wave or diffracted fields in PTD as expressed in (3), the hybrid method gives fields which are numerical analysis to exact one for practical problems.

First, this section is outlined, which is followed by a comparison between PO and PTD in the near-in angular region and far angular region. The PO envelope errors are estimated by comparing it with PTD and are noted by PO/PTD envelope error.
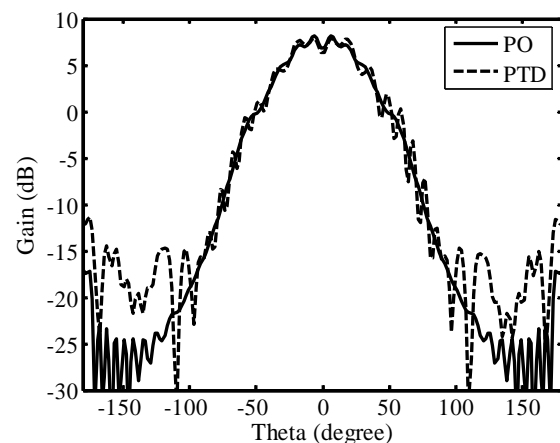
(a) E-plane
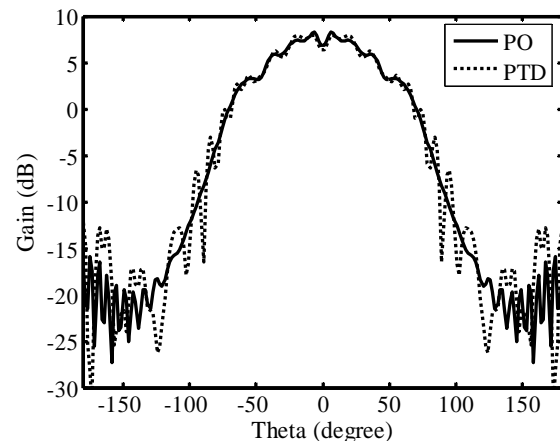
(b) H-plane

Fig. 9 Comparison of calculated patterns by PO and PTD.

A quadratic reflector is chosen with diameter $D = 30$ cm and feeding distance $f = 17$ cm (produces -10 dB edge illumination). The field patterns in E- and H-plane are calculated by PO and PTD as illustrated in Fig.9. It is found that in the near-in angular region, the PO and PTD are in perfect agreement. This is because PO currents are set to

zero in the shadowed region, creating shadow boundary on the reflector surface. In addition, the discontinuity of the current density over the rim of reflector is neglected. These approximations lead to accurate results for the radiated fields on the near-in angular region. As we can see in Fig.10, the envelope error at $0° \leq \theta \leq 10°$ of E- and H-plane patterns are lower than 0.5 dB. To predict the pattern more accurately in all regions, especially the far angle region, diffraction techniques can be applied. It is commonly argued that the field pattern results by PTD yield the accuracy more than by PO method, especially, in the far angular region. It is also observed that, the field patterns in the E- and H-plane, which are predicted by PTD, yielding the far-field envelope higher than by PO method.
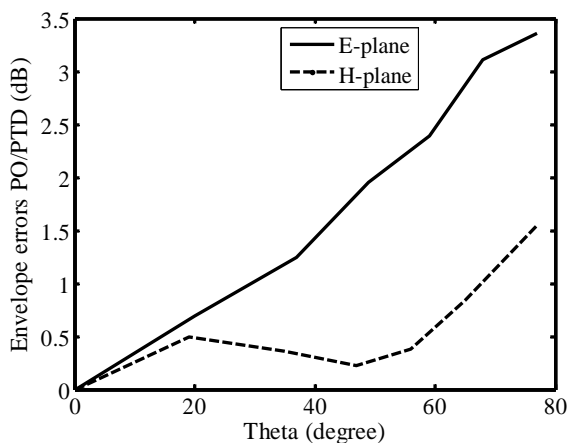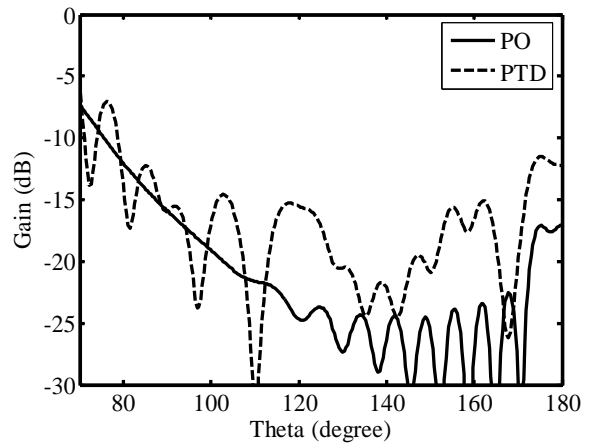

(a) E-plane

Fig. 10 PO/PTD envelope errors.

Although the patterns in Fig.9 at first sight look identical but there are in fact discrepancies in the region behind the reflector, i.e. for $70° \leq \theta \leq 180°$. In Fig.11, the discrepant region is zoomed to illustrate the difference of calculated results by PO and PTD. It is found that the results by using this two methods clearly disagree by as much 10 dB on some of the lobes for E- plane and as much 5 dB for H-plane. In the shadow region, the total field is generated by a superposition of the diffracted field from reflector as illustrated in Fig.12 and direct field from the feed; it is of utmost importance that correct model is used since otherwise it will not be possible to make the two contributions cancel out.
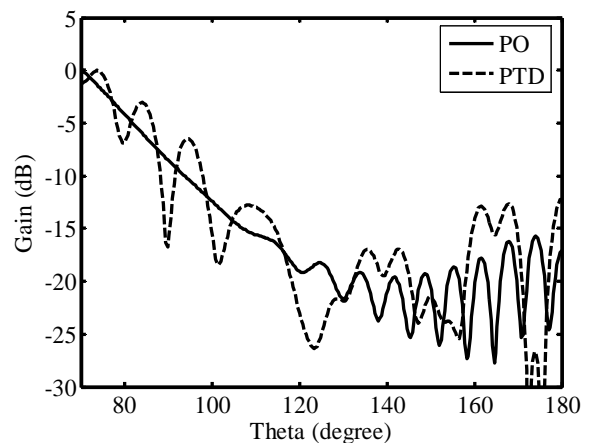
(b) H-plane

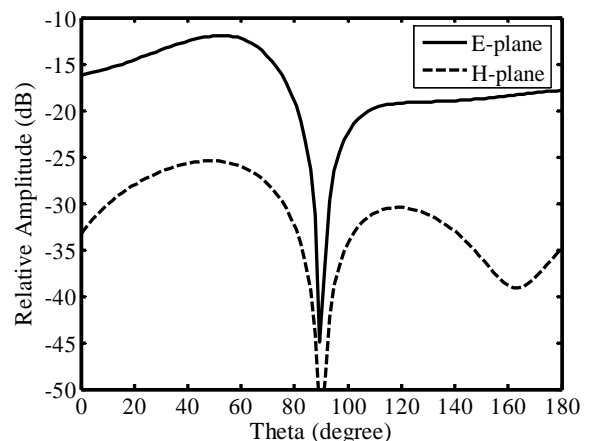Fig. 11 Close look at the rear pattern in E- and H-plane.

Fig. 12 Diffracted field patterns in E- and H-plane.

5 Experimental Results

To verify the radiation characteristics, the experiment was set up at the frequency of 10 GHz (available equipments) to measure the E- and H-plane radiation patterns. The dimension of quadratic reflector having $D = 30$ cm, feeding distance $f = 17$ cm. The quadratic reflector is duplicated to the curve surface by using the computer-numerically controlled (CNC) machine.


Fig. 13 Far-field pattern measurement of antenna in anechoic chamber.

The radiation patterns were measured in an anechoic chamber using vector network analyzer HP 8722D and standard X-band horn as shown in Fig.13. The measurement set up comprises two antennas, faced together at far field distance ($R > 2D^2 / \lambda$). Fig.14(a)-(b) show, respectively, the far-field patterns of quadratic reflector antenna in E-plane and H-plane pattern, and compared to the simulated results, which are calculated by using PO and PTD. Because of the feed blocking effect by simulation are neglected, therefore, the dip in pattern boresight from measurement of around 4 dB are occurred. Nevertheless, we found that the small ripple appears on the envelope of measured patterns, which are caused from some multipath effect that provided by construction of feed horn and metallic masts. Furthermore, if we compare the average levels on the all curves of each plane in far angle region, it will be observed that a difference from measured pattern on the order of 1 dB approximately for PO and 0.3 dB for PTD. It is seen that PO has the error more than PTD when compared its calculated results with measured results. This is attributed that no including the effects of edge diffraction into the field calculation by PO method. However, the agreement between simulated and measured results is satisfactory. In Table 3, the verification between simulation and experiment has been presented in the parameters of

maximum gain and HPBW. The maximum gain of simulated results by using PO in E- and H-planes pattern are higher than measured results around 0.18 dB and 0.02 dB, respectively, while the maximum gain of simulation by using PTD are higher than measured results around 0.13 dB and 0.01 dB, respectively. Besides that the measured results of HPBW are wider than the simulated results around 4° in E-plane and 2° in H-plane for PO and around 2° in E-plane and 1° in H-plane for PTD. Therefore, it can be summarized that the maximum gain and HPBW between simulated and measured results can show some minor differences both in E- and H-plane patterns. An additional cause of asymmetry observed in the measured patterns is (the combination of) the small defocusing and mispointing of the feed, i.e., feed displacements and tilts.
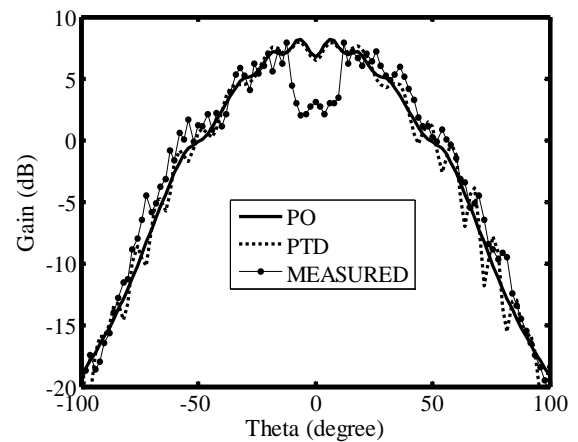
(a) E-plane
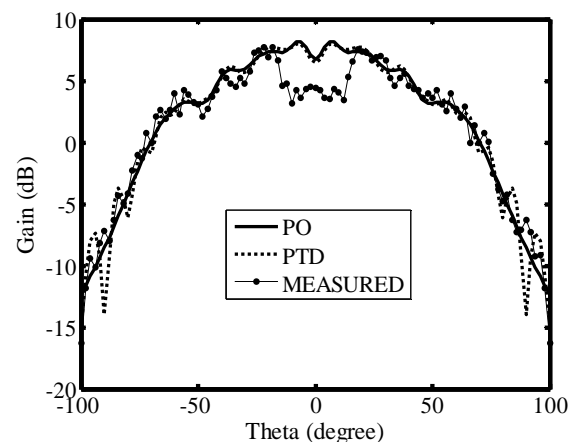
(b) H-plane

Fig. 14 Far field pattern for quadratic reflector.

Table 3
Comparison of simulated and measured results
for antenna characteristics

Antenna characteristics	E-plane	H-plane
Maximum gain (PO)	8.20 dB	7.76 dB
Maximum gain (PTD)	8.05 dB	7.75 dB
Maximum gain (measured)	7.92 dB	7.74 dB
HPBW (PO)	66°	98°
HPBW (PTD)	68°	99°
HPBW (measured)	70°	100°

6 Conclusion

The numerical study on the radiation pattern of various reflector shapes by using backscattering technique to provide broad-beam pattern can be obtained. The shapes of reflectors are determined from various functions of elementary geometries. PO is used for synthesis radiation pattern characteristics i.e., maximum ripple level, maximum gain, and HPBW of the reflector shapes. From all the aforementioned of radiation characteristics, it can be summarized that these reflector shapes can be chosen according to the characteristic requirements in practical applications. It is found that, the quadratic curvature of reflector will provide the optimum characteristics than other curvatures for large-scale indoor wireless LAN application. Therefore, the quadratic reflector are analyzed into detail by introducing the fringe wave in PTD, this hybrid method gives fields which are numerical analysis to exact one for practical problems. The antenna prototype with quadratic reflector was fabricated by high-precision CNC machine and measured field patterns in anechoic chamber. Good agreement between simulated and measured results is obtained. Finally, we can conclude that this proposed antenna exhibits moderate gain and excellent radiation coverage. These features make this antenna suitable for point-to-multipoint communications, especially, wireless LAN system and LEO satellite.

References:
[1] E.A. Rachid, M. Meouchy and G. Chdchany, Study, Synthesis, and Measurements of New Designs for WLAN Antennas, *WSEAS Transactions on Communications*, Vol.6, No.1, 2007, pp. 80-85.

[2] H. Elsadek, D. Nashaat and H. Ghali, Broad-ban U-Shaped PLFA with Dual band Capability for Bluetooth and WLAN Applications, *WSEAS Transactions on Computers*, Vol.3, No.6, 2004, pp. 1788-1793.

[3] G. Tsachtsiris, M. Karaboikis, C. Soras, V. Papamichael and V. Makios, Multi Element Fractal Rectangular Curve Patch Antenna for Indoor Access Points, *WSEAS Transactions on Communications*, Vol.3, No.2, 2004, pp. 478-481.

[4] P. Krachodnok and R. Wongsan, Design of Broad-Beam Microstrip Reflectarray, *WSEAS Transactions on Communications*, Vol.7, No.3, 2008, pp. 180-187.

[5] S.G. Hay, D.G. Bateman, T.S. Bird, and F.R. Cooray, Simple Ka-band Earth Coverage Antennas for LEO Satellites, *IEEE Antennas Propag. Soc. Int. Symp.,* Vol.1, 1999, pp. 11-16.

[6] T.S. Bird, J.S. Kot, N. Nikolic, G.L. James, and S.J. Barke, Millimeter-Wave Antenna and Propagation Studies for Indoor Wireless LANs, *Antennas Propag. Soc. Int. Symp.*, Vol.1, 1994, pp. 336-339.

[7] P.F.M. Smulders, S. Khusial, and M.H.A.J. Herben, A Shaped Reflector Antenna for 60-GHz Radio Access points, *IEEE Trans. on Antenna and Propag.*, Vol.49, 2001, pp. 1013-1015.

[8] P.F.M. Smulders, S. Khusial, and M.H.A.J. Herben, A Shaped Reflector Antenna for 60-GHz Indoor Wireless LAN Access points, *IEEE Trans. on Vehicular Technology*, Vol.50, 2001, pp. 584-591.

[9] A. Kumar, Antenna for Wireless Indoor Millimeter-Waves Applications, *Proc IEEE CCECE*, Vol.3, 2003, pp. 1877-1880

[10] D.W. Duan, Y.R. Samii and J.P. Mahon, Scattering from a Circular Disk: A Comparative Study of PTD and GTD Techniques, *Proc IEEE*, Vol.79, 1991, pp. 1472-1480

[11] P.Y. Ufimtsev, Method of Edge Waves in the Physical Theory of Diffraction, Izd-Vo Sovyetskoye Radio, pp. 1-243. (Translation prepared by the U.S. Air Force Foreign Technology Division Wright Patterson, AFB, OH, 1971; available from NTIS, Springfield, VA 22161, AD733203)

[12] M. Ando, Radiation Pattern Analysis of Reflector Antennas, *IEICE Trans.* (Japanese Edition), Vol.J67-B, No. 8, 1984, pp. 853-860.

[13] K.M. Mitzner, Incremental Length Diffraction Coefficients, Aircraft Division Northrop Corp., Tech. Rep. AFAI-TR, 1974, pp. 73-296.

[14] A. Michaeli, Equivalent Edge Currents for Arbitrary Aspects of Observation, *IEEE Trans.*

Antennas and Propag., Vol.AP-32, 1984, pp. 252-258.

[15] E.F. Knott, The Relationship Between Mitzner's ILDC and Michaeli's Equivalent Currents, *IEEE Trans. Antennas and Propag.*, Vol.AP-33, 1985, pp. 112-114.

[16] V. Thaivirot and R. Wongsan, Diffraction Analysis of a Quadratic Backscatter Antenna Using Physical Optics and Physical Theory of Diffraction, *Proc. ISAP2007*, 2007, pp. 197-200.

[17] A. Michaeli, Elimination of Infinities in Equivalent Edge Currents, Part I: Fringe Current Components, *IEEE Trans. Antennas Propag.*, Vol.AP-34, 1986, pp. 912-918.

[18] V. Thaivirot, P. Krachodnok and R. Wongsan, The Numerical and Experimental Study of Radiation Pattern from Various Shaped Reflectors Base on PO and PTD methods, *7th WSEAS International Conference on Applied Computer & Applied Computational Science (ACACOS' 08)*, 2008, pp. 54-59.